Measurement of the Kuroshio and its Associated Luzon Strait throughflow by Ocean Acoustic Tomography

Arata Kaneko,
Professor
Graduate School of Engineering
Hiroshima University
1-4-1 Kagamiyama, Higashi-Hiroshima 739-8527, Japan
TEL/FAX: +81-082-424-7625
E-mail: akaneko@hiroshima-u.ac.jp

N000140810139

INTRODUCTION

The Luzon Strait is a key place in the East Asian climate change study. The climate condition of the South China Sea is significantly controlled by the Luzon Strait transport (LST) (Qu et al., 2004; Liu et al., 2008). Variability in the Kuroshio origin around the strait is mostly caused by the LST, and significantly affects the oceanic variability around Japan and Korea in the downstream. In spite of the importance of LST measurement, most of the previous observations are based on hydrography (Nitani, 1972; Shaw, 1991; Chen and Huang, 1996; Yaremchuk et al., 2009), and the direct measurement of current is still limited in the observational period and spatial coverage (Y. Yuan et al., 2008; Liang et al., 2008).

The ocean acoustic tomography (OAT) is a powerful tool that can estimate the structure of sound speed (mainly proportional to temperature) and current in the ocean (Munk et al., 1995). While a lot of effort has been devoted to sound speed structure measurement, application of OAT to current structure measurement is still restricted to the coastal seas (Park and Kaneko, 2000; Yamaguchi et al., 2005 and Lin et al., 2005). The OAT has never been applied in oceans characterized with strong internal tides and waves like the Luzon Strait (Niwa and Hibiya, 2004). This may be caused by that the sound transmission in such oceans interacts strongly with these tides and waves and is unexpectedly disturbed not to obtain an accurate result of temperature and current.

A long-term OAT experiment for current measurement is attempted at the northern part of the Luzon Strait where the Kuroshio-related current and the strong internal tides and waves occur. Four-month observation results are presented together with the new clock correction method and compared with the moored upward-looking acoustic Doppler current profiler (ADCP) data.

OBSERVATION

A middle-range OAT experiment composed of three mooring stations (T1, T2 and T3) was carried out with range about 36km at the northern part of Luzon Strait during April to September 2008 (Fig. 1). The floor depth ranges from 900m to 1700m around the tomography site. The 800Hz organ pipe transducer (Engineering Acoustic Inc.) is attached at depth 800m on the subsurface mooring line for all stations and transmits one

Report Documentation Page

Form Approved
OMB No. 0704-0188

1. REPORT DATE	2. REPORT TYPE	3. DATES COVERED
SEP 2009	**Annual**	**00-00-2009 to 00-00-2009**

4. TITLE AND SUBTITLE
Measurement Of The Kuroshio And Its Associated Luzon Strait Throughflow By Ocean Acoustic Tomography

5a. CONTRACT NUMBER
5b. GRANT NUMBER
5c. PROGRAM ELEMENT NUMBER

6. AUTHOR(S)

5d. PROJECT NUMBER
5e. TASK NUMBER
5f. WORK UNIT NUMBER

7. PERFORMING ORGANIZATION NAME(S) AND ADDRESS(ES)
Hiroshima University,Graduate School of Engineering,1-4-1 Kagamiyama, Higashi-Hiroshima 739-8527, Japan,

8. PERFORMING ORGANIZATION REPORT NUMBER

9. SPONSORING/MONITORING AGENCY NAME(S) AND ADDRESS(ES)

10. SPONSOR/MONITOR'S ACRONYM(S)
11. SPONSOR/MONITOR'S REPORT NUMBER(S)

12. DISTRIBUTION/AVAILABILITY STATEMENT
Approved for public release; distribution unlimited

13. SUPPLEMENTARY NOTES
Code 1 only

14. ABSTRACT
The Luzon Strait is a key place in the East Asian climate change study. The climate condition of the South China Sea is significantly controlled by the Luzon Strait transport (LST) (Qu et al., 2004; Liu et al., 2008). Variability in the Kuroshio origin around the strait is mostly caused by the LST, and significantly affects the oceanic variability around Japan and Korea in the downstream. In spite of the importance of LST measurement, most of the previous observations are based on hydrography (Nitani, 1972; Shaw, 1991; Chen and Huang, 1996; Yaremchuk et al., 2009), and the direct measurement of current is still limited in the observational period and spatial coverage (Y. Yuan et al., 2008; Liang et al., 2008).

15. SUBJECT TERMS

16. SECURITY CLASSIFICATION OF:			17. LIMITATION OF ABSTRACT	18. NUMBER OF PAGES	19a. NAME OF RESPONSIBLE PERSON
a. REPORT	b. ABSTRACT	c. THIS PAGE			
unclassified	**unclassified**	**unclassified**	**Same as Report (SAR)**	**10**	

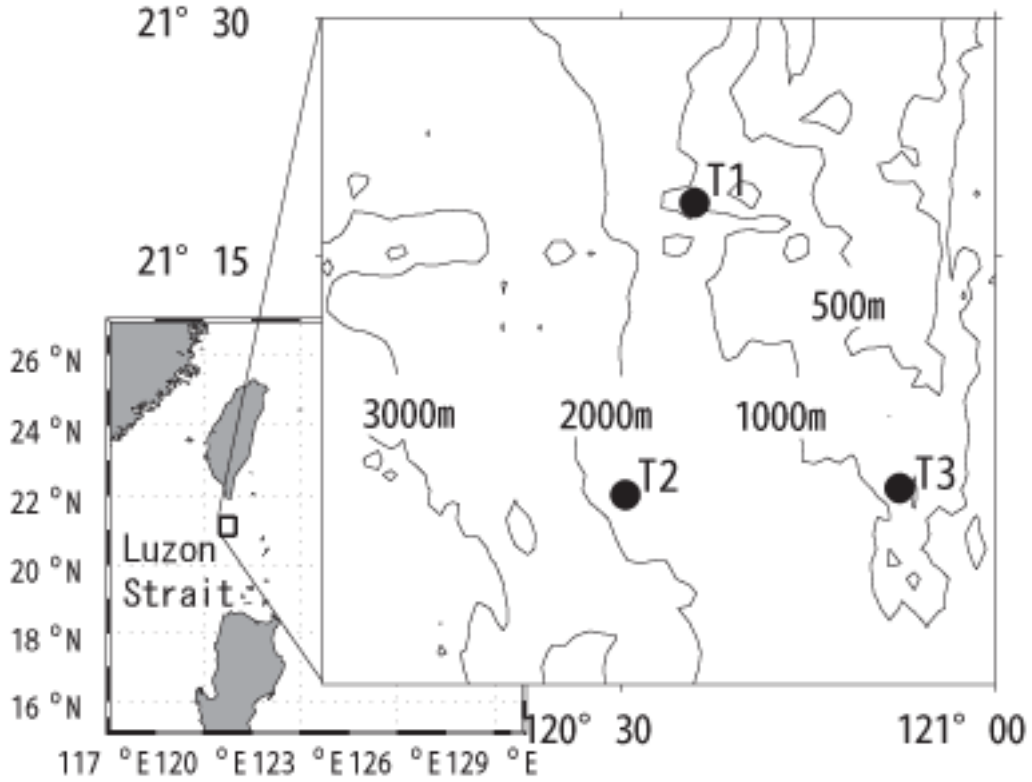

Fig. 1 Location map of the observation site. The bathymetric chart is shown in a magnified scale on the right side of the figure. T1, T2 and T3 are the mooring stations equipped with the OAT system. T1 and T2 also equip the upward-looking moored ADCP at the top of the mooring line.

period (about two minutes) of the 12th order M sequence every eight hours. The eight-hour data are smoothed through the 14-day running mean to filter out the tidal variation and focus on stable ocean currents like the Kuroshio.

The transducer is a narrow band one with a frequency range of 25Hz while the conventional acoustic tomography experiments always have used broad-band transducers. This forces us to shift to the cycle-per-digit value of 24 from 4 suitable for the conventional experiment. The power of sound transmission can be considerably reduced in the operation of narrow-band transducer. This provides a big advantage for the long-term operation of the subsurface tomography system by reducing the battery consumption. The deployment and recovery works were performed onboard the R.V. Dong Fang Hong of the Ocean University of China. The four-month data were successfully acquired for the stations T1 and T2 while the T3 mooring could not be recovered by the troubles which may be caused by fishing nets. Note that the top float of the mooring line is located at depth 150m for T3 in contrast to T1 and T2 at depths 600m and 300m, respectively.

The moored upward-looking ADCP (RDI-SC Narrow-Band for T1 and RDI-SC Workhorse Long Ranger for T2) is attached at the top of the mooring lines T1 and T2 for comparing with the OAT data. The working frequencies of ADCP are 150kHz and 75kHz for T1 and T2, respectively. Unfortunately the T1-ADCP was suddenly stopped in one and half months after the deployment because of the

system trouble. The raw ADCP velocities, acquired with bin lengths of 8m and 20m for T1 and T2, respectively are also smoothed by the two-day running mean (T1) or 40-h Butterworth low-pass filter (T2) to remove the semi-diurnal and diurnal tides. A number of CTD casts were done around the tomography site at the deployment and recovery cruises to know the sound speed fields.

Clock correction

Special attention is here paid on the accurate measurement of ocean current which requires highly precise clock. The OAT system is equipped with a timing module, composed of GPS (global positioning system) clock, quartz clock (SeaScan, Time Base Module) and Rubidium clock (TEMEX TIME, MCFRS-01). The quartz clock is always operated as an internal clock with calendar during the experiment. The internal clock is synchronized with the GPS clock immediately before the deployment into water and the drift of the internal clock is measured in comparison with the GPS clock immediately after the recovery from water. The Rubidium clock is operated during the first day after the deployment and compared with the internal clock to estimate the drift rate per second. The internal clock is corrected with this drift rate before the next transmission. This procedure of clock correction is well operated during the whole observation. However the resulting clock drifts make several hundred milliseconds much greater than the expected ones of ten milliseconds. This clock drift is too big to estimate ocean currents in a 36km range with a satisfactory accuracy of about 5cm/s. The new clock correction method is here proposed to replace the timing module method. When an acoustic transducer is located near the axis of the underwater sound channel (USC), some acoustic rays advance near the USC axis with no current. This requires that travel time differences are zero for these rays. By using this assumption, the time-wise growth of clock correction (Δt) is formulated with the following regression curve:

$$\Delta t = -0.0018\hat{t}^5 + 0.0028\hat{t}^4 - 0.0001\hat{t}^3 + 0.0102\hat{t}^2 + 0.1960\hat{t} + 0.2553$$

$$\hat{t} = \left(t - Mean(t)\right)/STD(t)$$

where t denotes the time in unit of hour elapsed from the deployment of the system into water and Δt the clock correction in unit of second at time t. The Mean(t) and STD(t) denote the mean and standard deviation of t, respectively The data scatter around the above line with a STD of 10.3ms, which corresponds to the velocity of 4.1cm/s. This velocity provides an error bar for the accuracy of the new clock correction method, proposed here.

Ray simulation and the sound transmission data

The sound transmission process between the stations T1 and T2 is simulated by the ray-tracing method, in which only the reflection and refraction of sound are considered. This is performed by using the range-averaged sound speed profile, estimated from all the acquired CTD data. The ray paths with bottom reflection numbers less than two are divided into three groups, shown with the ray diagram in Fig. 2. The travel times for the rays are plotted against the launch angles at lower middle of the figure. The first arrival group (Ray-1) makes travel times around 23.9s. Also the arrival times for the second (Ray-2) and third (Ray-3) arrival groups are around 24.0s and 24.1s, respectively. Ray- passes the depth range of 500-1300m. Ray-2 and Ray-3 reach the 200m layer at the northern two-third of the section while they are quite different at the southern one-third of the section where Ray-2 draws a downward sloping line and Ray-3 an upward convex curve.

The transmission signals at the stations T1 and T2 are phase-modulated with the 12th order M sequence of different codes. The received data at the stations T1 and T2 are cross-correlated with the same codes of the 12th order M sequence, used in the transmission at T1 and T2 to increase the signal-to-noise ratio (SNR). The travel time of acoustic ray between the stations T1 and T2 can be determined from the significant arrival peaks which exist in the correlation waveform. As shown typically in the left

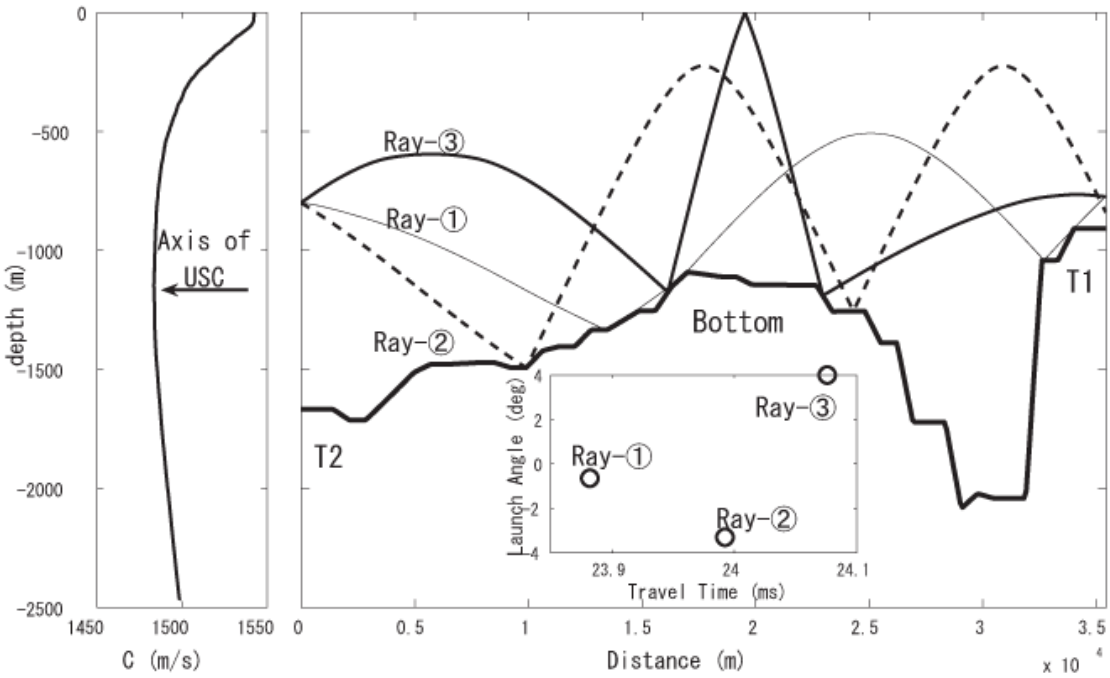

Fig. 2 Result of the ray simulation. The average vertical profile of sound speed, used in the simulation is calculated from all the CTD data and shown at the left of the figure. The bottom reflected rays with reflection numbers less than two are drawn. At the lower middle of the figure, the travel times are plotted against the launch angles at T2. The ray paths with travel times around 23.9s, 24.0s and 24.1s are named Ray-1, Ray-2 and Ray-3, respectively. Ray-1, Ray-2 and Ray-3 are drawn with the thin solid line, the thick dashed line and the thick solid line, respectively.

panel of Fig. 3, there are several arrival peaks in each of correlation waveforms, acquired every eight hours. We here focus on three arrival peaks distributing in the travel-time range from 23.9s to 24.1s. These arrival peaks are identified as ray groups for the first, second and third arrivals. In comparison with Figure 2, these arrival rays are likely to correspond to Ray-1, Ray-2 and Ray-3. The significant arrival peaks sometimes exist at 24.2s and more, but these data corresponding to rays with multi reflections at the surface and being less coherent are not used in the following analyses.

All the correlation waveforms obtained originally at the stations T1 and T2 are stacked with the transmission time going upward as shown at the right panel of Fig. 3.

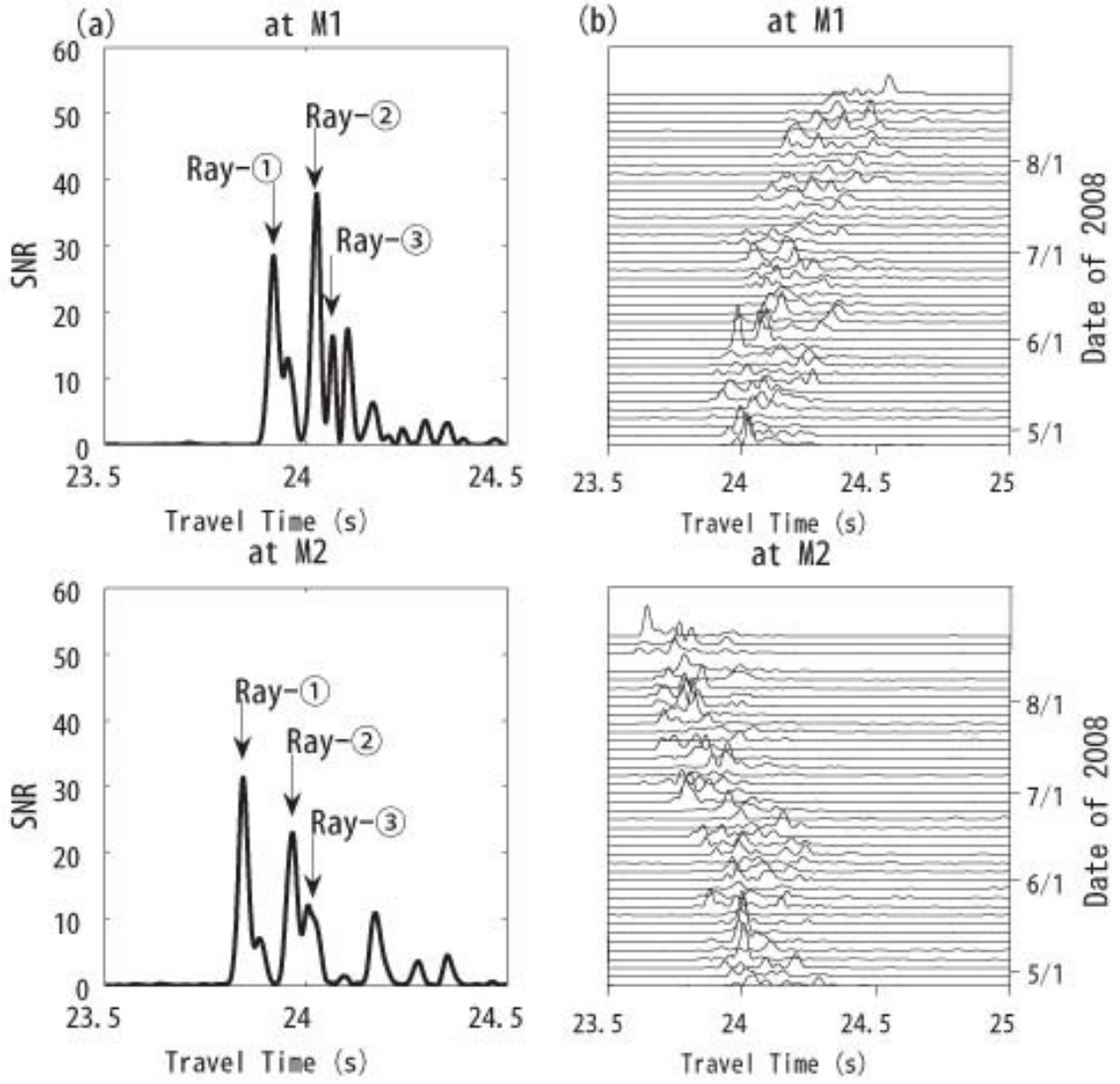

Fig. 3 Typical correlation waveforms obtained at T1 and T2 (left panel) and the stack diagrams for the T1 and T2 data, re-sampled every three days (right panel). The arrival peaks corresponding to Ray-1, Ray-2 and Ray-3 are pointed out with the downward arrows.

This is the result before clock correction. Arrival peaks are visible as a wave packet on the correlation waveform. The wave packets are shifted continuously with the transmission time. The internal clock of T1 and T2 makes a reverse tendency of clock drift: the T1 clock goes ahead and T2 clock is delayed. The necessity of clock correction is well understood as seen by the large drift of the internal clock.

Velocity data and comparison with other data

The correction rate of internal clock are determined by putting the travel time difference for Ray-1 into zero. The corrected travel time differences (Δt) for Ray-2 and Ray-3 are converted into the range-averaged velocities (u_m), obeying the following formula (Zheng et al., 1997):

$$u_m = \frac{c_m^{\,2}}{2L}\Delta t$$

where L denotes the horizontal distance between the stations T1 and T2. The range-averaged velocities for Ray-2 and Ray-3, smoothed through the 14-day running mean are shown with the time plots in Fig. 4. During the beginning of May to the middle of July, the average velocities are directed toward T1 from T2 (positive) and vary in the range of 0-10 cm/s and 5-15 cm/s for Ray-2 and Ray-3, respectively. After that, they start to decrease suddenly and make a reverse current (directed from T1 to T2), centered at the beginning of August. During the reverse current. both the velocities are almost the same.

The ADCP data, obtained at the stations T1 and T2, are also shown in Figure 4 with the time plots. The three layered velocities of 100-200m, 200-300m and 300-400m are shown for the T2-ADCP data while only the 100-200m layer velocity is shown for the T1 -ADCP data. Both the ADCP data for the 100-200m layer are in good agreement. The T2-ADCP data shows a significant vertical shear of current until the middle of July. However this large shear is suddenly diminished in the period of reverse current, centered at the beginning of August and all the OAT and ADCP velocities are coincident.

Summary and discussion

The ocean acoustic tomography experiment is carried out at the northern part of the Luzon Strait with an aim of the long-term measurement of ocean current. The timing module composed of GPS, Quartz and Rubidium clocks is well operated、but the expected performance is not attained. The accurate analysis of the long-term current data is accomplished under the new clock correction method in which the correction rate is determined by putting the travel time difference for rays passing near the USC axis into zero. Information on ocean dynamics that currents are generally very weak at the bottom of the permanent thermocline, namely the axis of USC, plays an essential role in the

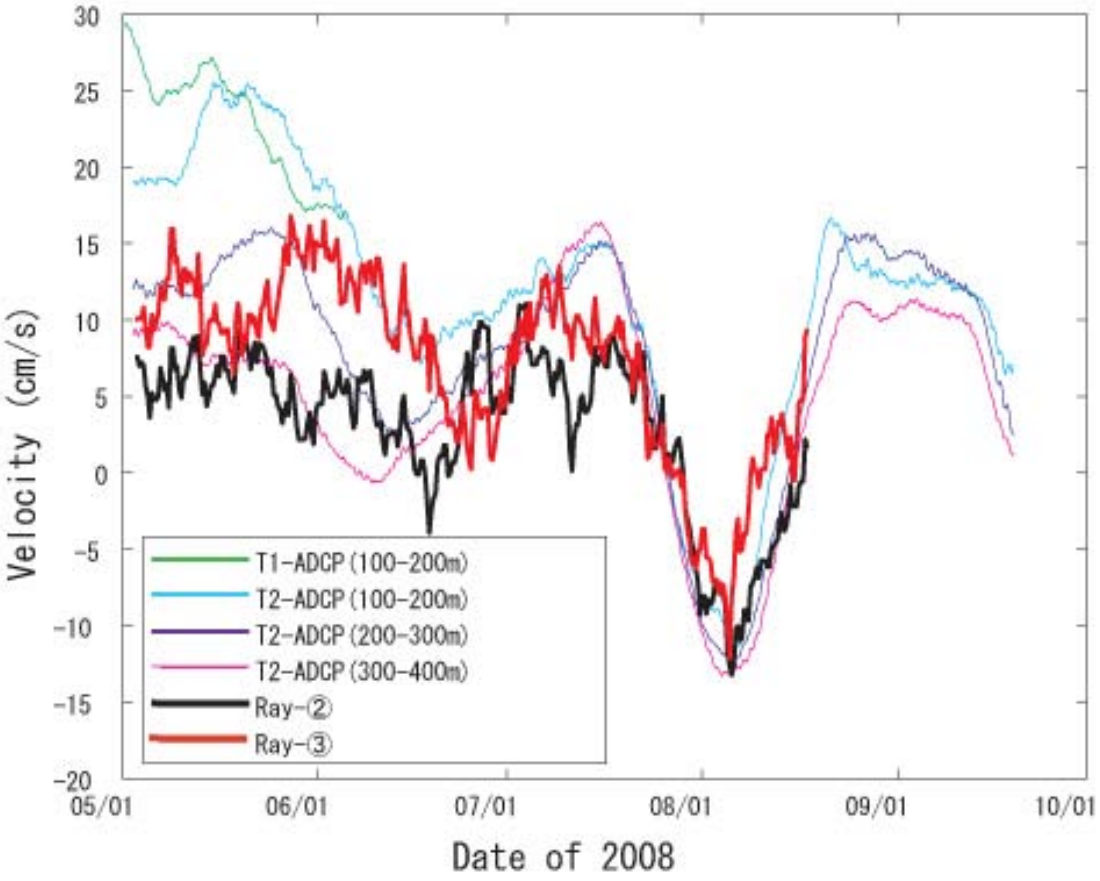

Fig. 4 OAT velocities for Ray-2 (thick black line) and Ray-3 (thick red line), compared with the ADCP velocities at 100-200m (thin blue line) , 200-300m (thin green line) and 300-400m (thin pink line) of T2 and at 100-200m (thin green line) at T1.

realization of this clock correction method. Yuan et al. (2008) reported the result of the moored current meter that mean currents acquired at depth 800m in the adjacent of the tomography site are as small as 1cm/s.

During the observational period from May to August 2008, the Kuroshio is likely to be located at the east of the tomography site, and then the OAT measures a relatively weak current less than 30cm/s at the western edge of the Kuroshio. On the other hand, the present OAT experiment is performed at the final phase of the 2007/08 La Nina (Pacific Marine Environmental Laboratory Web Site, http://www.pmel.noaa.gov/tao/ jsdisplay/). Qu et al. (2004) shows from the high-resolution ocean circulation model that the Luzon Strait transport (LST) becomes maximum during the El Nino year and minimum during

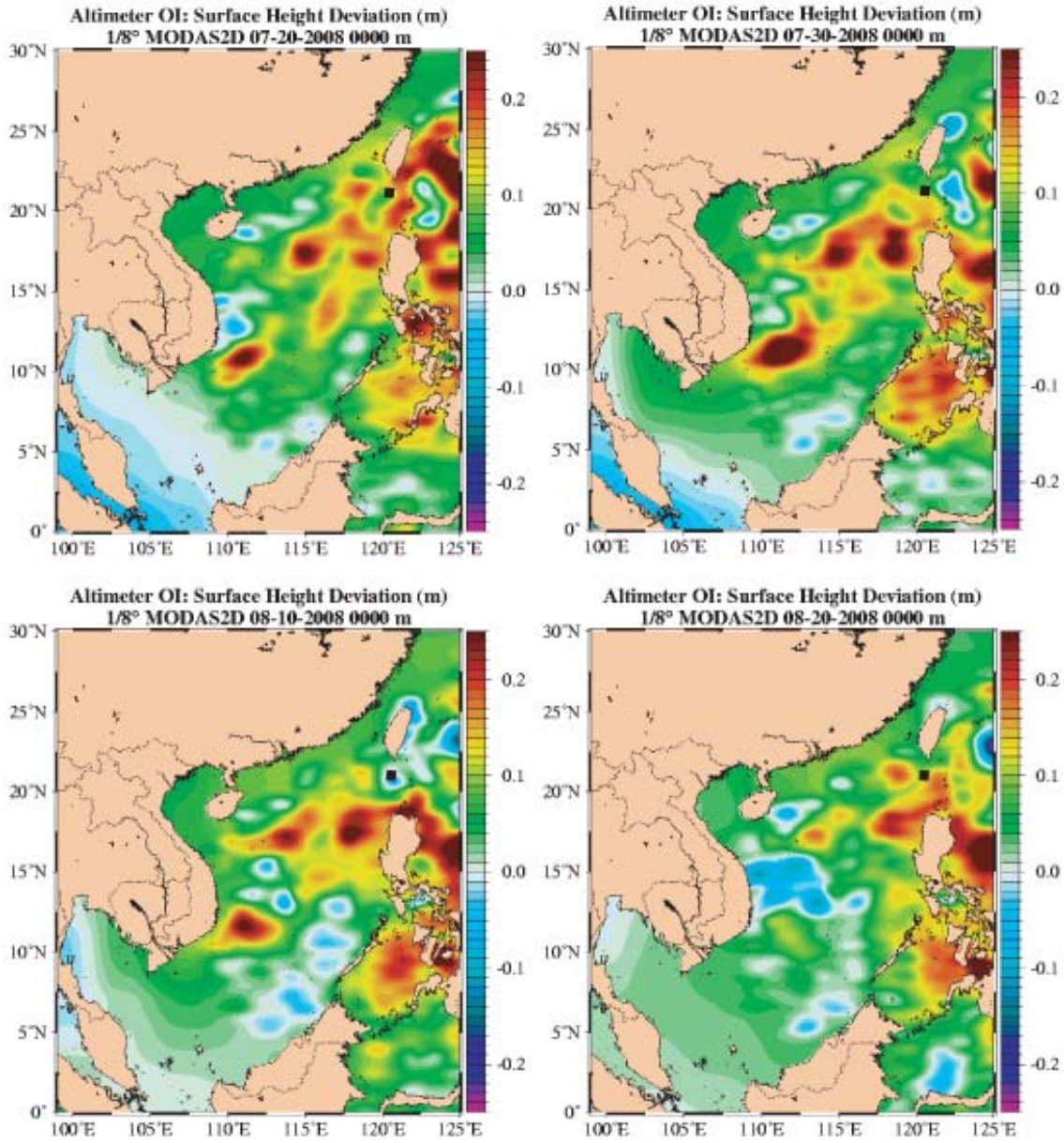

Fig. 5 Sequential maps of the satellite altimeter data, taken around the observation site on (a) July 20, (b) July 30, (c) August 10 and (d) August 20. The transmission line T1 - T2 is drawn with a solid square, placed at the south of Taiwan.

the La Nina year. Furthermore during the La Nina years the southward shift of the North Equatorial Current (NEC) bifurcation occurs and the Kuroshio is less intruded into the Luzon Strait with increased transport (Qu and Lukas, 2003). This is the reason why the tomography site is located further west of the stream axis of the Kuroshio. The ocean circulation modeling work also shows that the LST takes seasonal variability to be maximum in January-February and minimum in June-July (Qu et al., 2000). This provides an additional cause that the Kuroshio takes the eastward-shifted stream path during the acoustic tomography experiment, done in late spring to summer.

At the overall view during the beginning of May to the middle of July, the OAT velocities averaged along Ray- and Ray- are significantly weaker than the ADCP velocities except the first half of June. This is caused by that the former velocities average the depth range from the 200m to the bottom (Ray-2) and from the surface to bottom (Ray-3) while the latter velocities average the depth range from 100m to 400m. In contrast, the OAT velocity produces an overestimate of about 5cm/s during the first half of June. During one month from mid July to mid August, all the observed velocities are surprisingly coincident, making the prominent reverse flows and diminishing the vertical shear. It is likely that a cyclonic (cold) eddy with baroclinicity exists between the tomography site and the Kuroshio in the Philippine Sea to generate this reverse current. Cold eddies on the Philippine Sea side of the Luzon Strait are visible in the sea surface height anomaly (SSHA) data on July 20, July 30 and August 10, retrieved from the Naval Research Laboratory Web Site (http://www7320.nrlssc.navy.mil/modas2d/) (Fig. 5,). Especially the cold eddies in Figures 5 (a) and (b) make a barrier to the intrusion of the Kuroshio into the South China Sea. The cold eddies are also reported to be found in the surface geostrophic current calculated from the combined data of the mean dynamic topography and the SSHA (Figure 11 of D. Yuan, 2006). It is reported that the mesoscale eddies impinge the Kuroshio east of Taiwan at an interval of 100 days (Yang et al., 1999). The cold eddy may force the Kuroshio to make the eastward shifted path on the eastern side of the eddy and the reverse current on its western side after the collision with the Kuroshio. However the detailed dynamics of Kuroshio-eddy interaction requires further study.

During the reverse current the OAT velocities, which include the current from the surface to bottom, agree well with the ADCP velocities for the upper 400m. This means that the cold eddy is characterized with a baroclinic structure and its velocity is almost diminished at depth 500m, corresponding to the shallowest point of Ray-1. This baroclinic structure of cold eddies is also roughly supported by the CTD section acquired at 25N (Zhu et al., 2008).

REFERENCES

Chen, C-T. and M.H. Huang, 1996, A mid-depth front separating the South China Sea water and the Philippine Sea water, ***J. Oceanogr.*, 52, 17-25.**

Liang, W-D., Y-J. Yang, T-Y. Tang and W-S. Chuang, 2008, Kuroshio in the Luzon Strait, *J. Geophys. Res.*, 111, C08048, doi:10.1029/2007JC004609.

Liu, Q., A. Kaneko and J. Su, 2008, Recent progress in studies of the South China Sea Circulation, *J. Oceanogr.*, 64(5), 753-762.

Lin, J., A. Kaneko, N. Gohda and K. Yamaguchi, 2005, Accurate imaging and prediction of Kanmon Strait tidal current structures by the coastal acoustic tomography data, *Geophys. Res. Lett.*, 32, L14607, doi:10.1029/2005GL022914.

Munk, W., P. F. Worcestor and C. Wunsch, 1995, Ocean Acoustic Tomography, *Cambridge Univ. Press*, Cambridge, 433pp.

Nitani, H., 1972, Beginning of the Kuroshio, In Kuroshio, Its Physical Aspects, ed. by H. Stommel and K. Yoshida, *University of Tokyo Press*, p.129-163.

Niwa, Y. and T. Hibiya, 2004, Three-dimensional numerical simulation of M2 internal tides in the East China Sea, *J. Geophys. Res.*, 109, C04027, doi:10.1029/2003JC001923, 2004.

Park, J-H. and A. Kaneko, 2000, Assimilation of coastal acoustic tomography data into a barotropic ocean model. *Geophys. Res. Lett.*, 27(20), 3373-3376.

Qu, T., H. Mitsudera and T. Yamagata, 2000, Intrusion of the North Pacific waters into the South China Sea, *J. Geophys. Res.*, 105, 6415-6424.

Qu,T and R. Lukas, 2003, The bifurcation of the North Equatorial Current in the Pacific, *J. Phys. Oceanogr.*, 33, 5-18.

Qu, T., Y. Kim, M. Yaremchuk, T. Tozuka, A. Ishida and T. Yamagata, 2004, Can Luzon Strait transport play a role in conveying the impact of ENSO to the South China Sea?, *J. Climate*, 17, 3644-3657.

Shaw, P. T., 1991, Seasonal variation of the intrusion of the Philippine Sea water into the South China Sea, *J. Geophys. Res.*, 96, 821-827.

Yamaguchi, K., J. Lin, A. Kaneko, T. Yamamoto, N. Gohda, H-Q. Nguyen and H. Zheng, A continuous mapping of tidal current structures in the Kanmon Strait, *J. Oceanogr.*, 61, 283-294, 2005.

Yang, Y., C-T. Liu, J-H. Hu and M. Koga, 1999, Taiwan Current (Kuroshio) and impinging eddies, *J. Oceanogr.*, 55, 609-617.

Yaremchuk, M., J. McCreary JR., Z. Yu and R. Furue, 2009, The South China Sea throughflow retrieved from climatological data, *J. Phys. Oceanogr.*, 39, 753-767.

Yuan, D., W. Han and D. Hu, 2006, SurfaceKuroshio path in the Luzon Strait area derived from satellite remote sensing data, *J. Geophys. Res.*, 111, C11007, doi:10.1029/2005JC003412.

Yuan, Y., G-H. Liao, W. Guan, H. Wang and R. Lou, 2008, The circulation in the upper and middle layers of the Luzon Strait during spring 2002, *J. Geophys. Res.*, 113, C06004, doi:10.1029/ 2007JC004546.

Zheng, H., N. Gohda, H. Noguchi, T. Ito, H. Yamaoka, T. Tamura, Y. Takasugi and A, Kaneko, 1997, Reciprocal Sound Transmission Experiment for Current Measurement in the Seto Inland Sea, Japan, *J. Oceanogr.*, 53, 117-127.

Zhu, X., J-H. Park and D. Huang, 2008, Observation of baroclinic eddies southeast of Okinawa island, *Sci. in China Ser. D - Earth Sci.*, 51(12), 1802-1812.